Two-Dimensional Superlattice: Modulation of Band Gaps in Graphene-Based Monolayer Carbon Superlattices

ARTICLE *in* JOURNAL OF PHYSICAL CHEMISTRY LETTERS · NOVEMBER 2012

Impact Factor: 7.46 · DOI: 10.1021/jz301325z

THE JOURNAL OF PHYSICAL CHEMISTRY Letters

Letter

pubs.acs.org/JPCL

Two-Dimensional Superlattice: Modulation of Band Gaps in Graphene-Based Monolayer Carbon Superlattices

Xiaoguang Luo,*[,†] Li-Min Liu,[‡] Zhenpeng Hu,[§] Wei-Hua Wang,[†] Wen-Xiong Song,[∥,‡] Feifei Li,[§] Shi-Jin Zhao,[∥] Hui Liu,[†] Hui-Tian Wang,[§] and Yongjun Tian[⊥]

[†]Department of Electronics, Nankai University, Tianjin 300071, China

[‡]Beijing Computational Science Research Center, Beijing 10084, China

[§]School of Physics, Nankai University, Tianjin 300071, China

[∥]Key Laboratory of Microstructures and Institute of Materials Science, Shanghai University, Shanghai 200072, China

[⊥]State Key Laboratory of Metastable Materials Science and Technology, Yanshan University, Qinhuangdao 066004, China

ABSTRACT: A novel carbon allotrope consisting of parallel zigzag and armchair chains alternatively each other (10 atoms/cell, named pza-C_{10}) was discovered. The calculated band gap of pza-C_{10} is 0.31 (0.71) eV with PBE (HSE06), and thus the new member of carbon family is a semiconductor. The pza-C_{10} sheet not only is thermodynamically more stable than the other known semiconducting carbon sheets, but also it can perfectly graft with graphene. The unprecedented properties of pza-C_{10} provide a new approach of modulating intrinsic band gap through forming graphene-based monolayer carbon superlattices (GSLs). The band gaps of GSLs with zigzag type of interface oscillate between semiconducting and semimetallic (mostly at the Dirac point) states as the number of zigzag chains increases, showing quantum size effect. The 2D superlattice achieved in GSLs opens a new strategy to design the crystal structures and modulate the electronic properties of 2D materials, nanoribbons, and nanotubes.

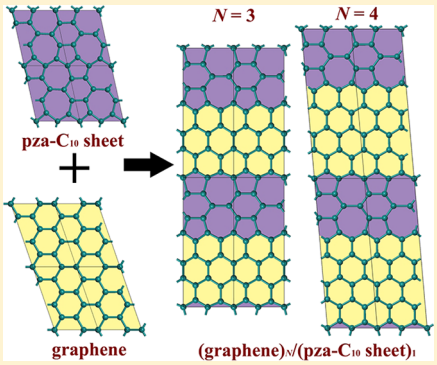

SECTION: Physical Processes in Nanomaterials and Nanostructures

Graphene has attracted considerable attention following the discoveries of massless Dirac fermions and quantum Hall effect in the system,[1−4] which has plenty of potential applications in high-performance graphene-based electronic devices. However, the zero band gap of pristine graphene has limited its device applications.[4] From the viewpoint of the physical potential, the opening of the band gap can be realized by applying an external potential to the graphene system, such as patterned hydrogen adsorption on the graphene,[5,6] interacting with substrates,[7−9] and applying electric fields to the graphene bilayers.[10−12] Although hydrogen adsorption and interaction with strong substrates can open the band gap of graphene, the intrinsic properties of graphene will also greatly decrease because of the strong chemical bonding. The band gap can be opened by only ∼0.3 eV through applying electric fields.[4]

Another approach to open the band gap of graphene is via the edge effects through forming the graphene nanoribbon (GNR),[13−16] which can be considered as applying additional boundary conditions to the graphene system. Although some large band gaps have been reported in GNR, it requires reducing the GNR width (band gaps of 0.5−3.0 eV needs the GNR width of 2.4−0.4 nm).[13,15] Recently, experimental and theoretical works have shown that band gaps can also be tuned by the neck width, periodicity of holes, and shape of lattice in graphene antidot lattices (GALs).[17−19] However, the nanometer scale holes in GALs, together with the edge effects, make the nature of GALs close to that of GNR.

It is a great desire to find an approach from both theoretical and experimental sides that not only keeps the intrinsic excellent electronic properties but also effectively opens the band gap of graphene. Superlattice is a widely used technique to modulate band structures and other physical properties of various materials.[20,21] Traditionally, superlattice is a periodic structure of layers of two (or more) materials that can be fabricated by alternately growing two thin films, forming a 1D periodic potential perpendicular to the growth direction in the multilayer films.[20,21] Since the rise of graphene,[4] a representative of 2D monolayer structures, it is natural to wonder whether we can extend the conventional superlattice of the quasi-2D system to the monolayer superlattice of the 2D system. To realize 2D superlattice in the graphene-related system, a 2D carbon allotrope should not only own an intrinsic band gap but also have excellent structure similarity with graphene. Although some 2D carbon allotropes, such as graphyne and graphdiyne, have been predicted or synthesized previously,[22−29] the reported semiconducting carbon sheets cannot be perfectly combined with graphene because most of such allotropes do

Received: September 1, 2012
Accepted: November 1, 2012
Published: November 1, 2012

   dx.doi.org/10.1021/jz301325z | J. Phys. Chem. Lett. 2012, 3, 3373−3378

Table 1. Typical Properties of the Novel Carbon Allotrope, pza-C_{10}, Compared with the Reported Semiconductor, Such As Graphyne, Graphdiyne, and C_{60}[a]

structure	space group no.	atoms per cell	ring per cell (n × ring)	E_d (eV/atom)	E_g (eV)	band gap type
graphene	191	2	6	0	0	Dirac point
graphyne	191	12	6 + 2 × 12	0.634	0.46	direct
graphdiyne[b]	191	18	6 + 2 × 18	0.771	0.49	direct
ref 27	191	12	3 × 4 + 2 × 6 + 12	0.637	0.03	direct
fullerene C_{60}		60	12 × 5 + 20 × 6	0.384	1.64	
ref 25	123	28	4 × 5 + 8 × 6 + 2 × 8	0.329	0.22	direct
pza-C_{10} sheet	10	10	2 × 5 + 6 + 2 × 7	0.250	0.31	indirect

[a]Relative energy E_d is defined as: $E_d = E_{carbon} - E_{graphene}$, where E_{carbon} and $E_{graphene}$ are the total energy per atom of the carbon allotrope and pristine graphene (unit: eV). As for rings per cell, rings indicates the total atom number of one ring, and n means the total number of the corresponding ring. For example, 12 × 5 + 20 × 6 denotes that the unit cell contains 12 pentagons and 20 hexagons, respectively. [b]Ref 28.

not own the zigzag or armchair chains. The formation of a perfect interface between graphene and alternative semiconducting carbon sheets for graphene-based monolayer-carbon superlattices (GSLs) is still an open question. To realize the 2D superlattice and modulate the band gap of graphene, new carbon allotropes with both moderate band gap and perfect structure similarity with graphene should be discovered.

In this manuscript, the carbon allotrope was thoroughly searched through a particle swarm structural search combined with DFT calculations. To this end, a novel 2D carbon allotrope was discovered. The new carbon structure contains 10 atoms/cell and two types of parallel blocks that consist of zigzag and armchair chains, and thus we named it pza-C_{10}. The new member, pza-C_{10}, of carbon family is thermodynamically more stable than the other known semiconducting carbon sheets and has surprisingly structural similarity with graphene, and thus it is a perfect material to graft with graphene to form 2D superlattices. The sp^2-hybridized pza-C_{10} sheet is a semiconductor, which can be regarded as specially arranged Stone–Wales (SW) defects in graphene. A series of GSLs was constructed by periodic insertion of pza-C_{10} sheets in the graphene lattice. Interestingly, the band gaps of the GSLs are greatly affected by both the chirality and width of graphene. In particular, the band gaps of the GSLs with zigzag type of interface oscillate between semiconducting and semimetallic (mostly at the Dirac point) states with the number of zigzag chains in its unit cell exhibiting quantum size effects. The intrinsic way to modulate band gaps through pure 2D GSLs will be helpful to further understand and design the 2D superlattices.

First, the structural search using CALYPSO code yielded almost all of the experimentally and theoretically known semiconducting 2D carbon sheets, as shown in Table 1.[22−28] Except such known semiconducting materials, an unexpected novel carbon sheet with a unit cell of 10 atoms was discovered, as shown in Figure 1a. The optimized lattice parameters are a = 4.63 Å, b = 6.02 Å, and γ = 102.4°. The unit cell of pza-C_{10} sheet is composed of two pentagons, one hexagon, and two heptagons with the space group of $P2/M$ (space group no. 10). All heptagons are connected periodically along the y axis, and the two connected pentagons are surrounded by two hexagons and four heptagons (Figure 1a), which can be considered to be specially arranged SW defects in graphene.[30] This new structure contains two types of parallel blocks that consist of zigzag and armchair chains in the structure, and thus it can perfectly match the lattice of graphene.

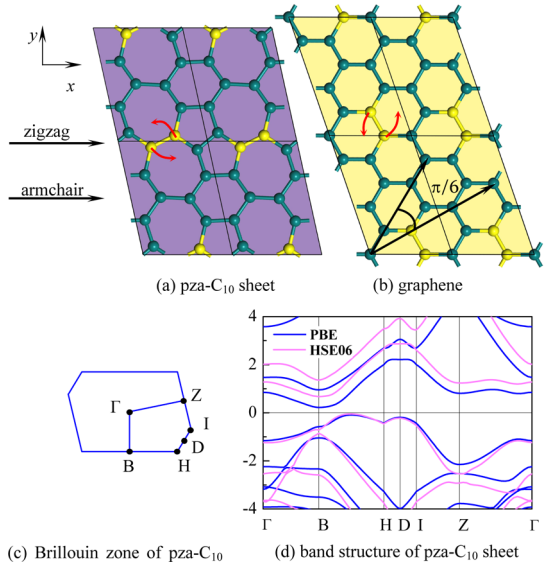

Figure 1. Crystal structures of the predicted pza-C_{10} sheet (a) and graphene (b); high-symmetry points in the first Brillouin zone (c) and the band structure (d) calculated with PBE and HSE06 functional of pza-C_{10} sheet. The Fermi level is indicated by the horizontal line. The directions of the armchair and zigzag chains are parallel to each other in the pza-C_{10} sheet, and thus the smallest angle between armchair and zigzag chains in graphene angle is $\pi/6$. The structure exchanges between graphene and pza-C_{10} sheet can be easily made by $\pi/2$ rotation of the C–C bond, as explained in yellow color and red arrows. The pza-C_{10} sheet can be considered as specially arranged SW defects or line defects in graphene. The indirect band gap of pza-C_{10} is 0.31 eV in PBE and 0.71 eV in HSE06 functional.

The stability of different carbon allotrope was calculated by energy difference between the allotrope and the graphene, which is defined as $E_d = E_{carbon} - E_{graphene}$, where E_{carbon} and $E_{graphene}$ are the total energy per atom of the carbon allotrope and pristine graphene, respectively. As shown in Table 1, the calculated E_d of the predicted pza-C_{10} sheet is 0.250 eV/atom, indicating that it should be a metastable phase relative to the graphene. It should be noted that the pza-C_{10} sheet is energetically the most stable one among reported semiconducting carbon sheets[25,27,28] and fullerene C_{60}. To check further the stability of the pza-C_{10}, a molecular dynamics simulation was conducted at 300, 900, 2100, and 3000 K, respectively. During the whole simulation times (25 ps), no structure change occurs, which suggests that the pza-C_{10} is thermodynamically stable.

dx.doi.org/10.1021/jz301325z | J. Phys. Chem. Lett. 2012, 3, 3373–3378

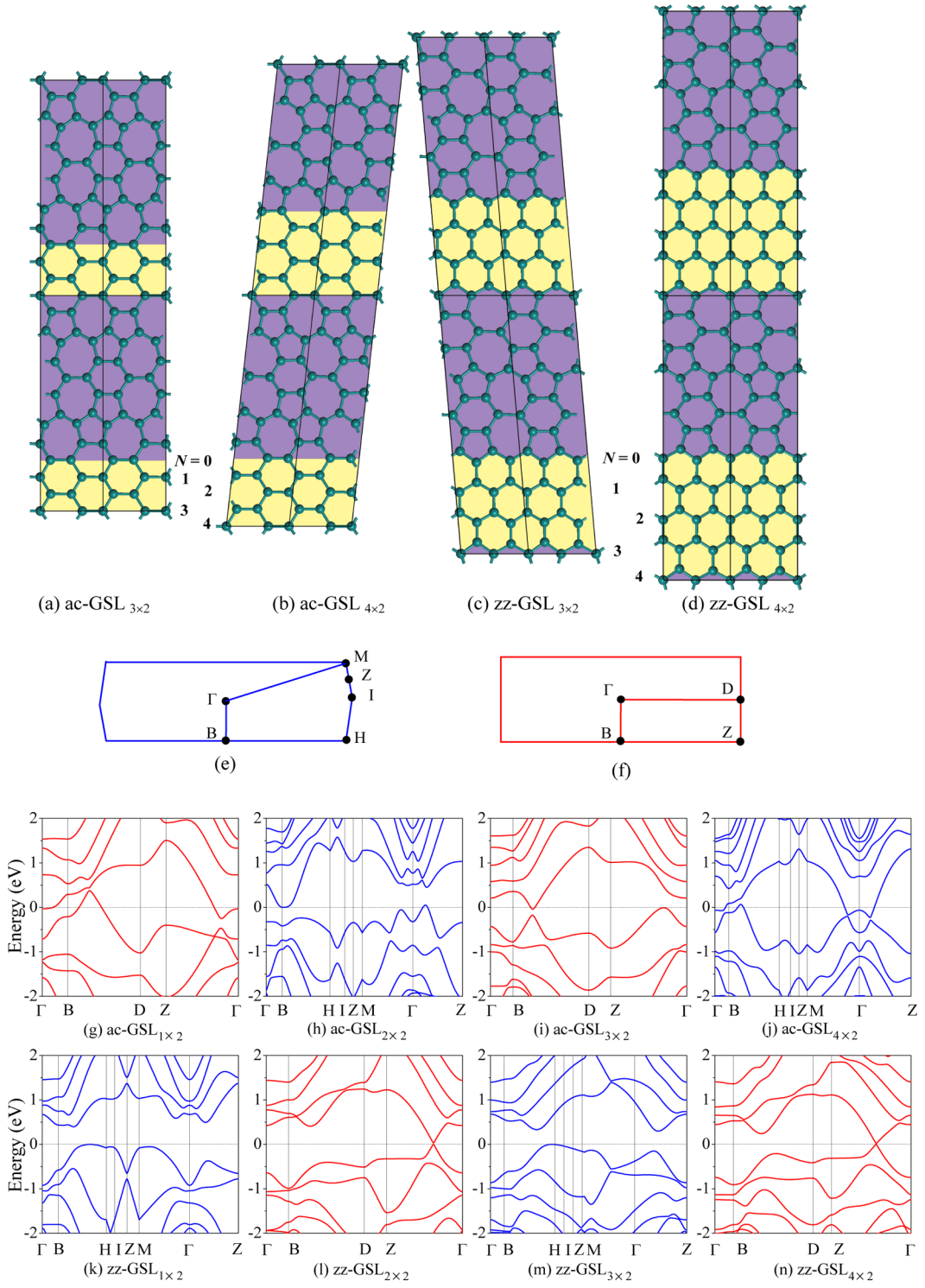

Figure 2. Typical crystal structures of ac-GSL$_{N\times2}$ and zz-GSL$_{N\times2}$, their first Brillouin zones, and band structures. (a) ac-GSL$_{N\times2}$ with odd number of chains, here N = 3; (b) ac-GSL$_{N\times2}$ with even number of chains, here N = 4; (c) zz-GSL$_{N\times2}$ with odd number of chains, here N = 3; (d) zz-GSL$_{N\times2}$ with even number of chains, here N = 4. The four typical structures represent that a class of GSLs are constructed by the various cutting and grafting between graphene and pza-C$_{10}$. The structures of GSLs and pza-C$_{10}$ have the same symmetry of $P2/M$. The Brillouin zone of the structures of ac-GSL$_{4\times2}$ (b) and zz-GSL$_{3\times2}$ (c) are shown in panel e. The Brillouin zone of the structure of ac-GSL$_{3\times2}$ (a) and zz-GSL$_{4\times2}$ (d) is shown in panel f. Band structures of ac-GSL$_{N\times2}$ with N = 1−4 and zz-GSL$_{N\times2}$ with N = 1−4 are shown in panels g−j and k−n, respectively. The band structures plotted with blue lines are calculated from the Brillouin marked as blue lines, whereas the band structures plotted with red lines are corresponding to the Brillouin marked as red lines.

As shown in Figure 1b, the unit of graphene supercell marked in black lines corresponds to the unit cell of pza-C$_{10}$ sheet (Figure 1a). Phase transition between graphene and pza-C$_{10}$ sheet can be achieved by the rotation of the C−C bond marked in yellow color, which is almost the same process as that of the typical SW phase transition in graphene. Previous theoretical

dx.doi.org/10.1021/jz301325z | J. Phys. Chem. Lett. 2012, 3, 3373−3378

calculations showed that SW defects in graphene can be generated by a $\pi/2$ in-plane rotation of two carbon atoms with respect to the midpoint of the bond,[22] accompanied by the breaking and reforming of two C−C bonds in a unit cell. Although a large energy barrier of 9.2 eV in this phase transition has been estimated by DFT calculations,[31] such kind of SW defects can be widely observed in the recent experiments of defect graphene or reduced graphene oxides.[32,33] Considering the high stability and structure similarity between pza-C_{10} and SW defect as discussed above, the pza-C_{10} sheet may be achieved using by the technique of bombing the graphene. Another possible way is that pza-C_{10} may be incorporated into the synthesis process of graphene.

The most interesting structural feature of the pza-C_{10} sheet is that both zigzag and armchair chains in pza-C_{10} are identical to those in graphene. The directions of the armchair and zigzag chains are parallel to each other in the pza-C_{10} sheet, whereas they have the smallest angle of $\pi/6$ in graphene. Owning such extraordinary structural character for the pza-C_{10}, many different types of 2D superlattices can be easily constructed using perfect combination of graphene and pza-C_{10} sheet. As shown in Figure 2a-d, typical GSLs of $(\text{graphene})_N/(\text{pza-}C_{10}\ \text{sheet})_M$ are built, where N and M are the integer numbers of armchair- or zigzag-chains blocks for graphene and the number of unit cells for pza-C_{10} sheet along the y axis, respectively. As discussed below, the band gaps of different $(\text{graphene})_N/(\text{pza-}C_{10}\ \text{sheet})_M$ fluctuate with the width of both graphene (N) and pza-C_{10} sheet (M). In the following, we mainly discuss how the widths of graphene (N) affect the band gap of the GSLs with the width of two unit cell of the pza-C_{10} sheet (M = 2). Hereafter, we name the $(\text{graphene})_N/(\text{pza-}C_{10}\ \text{sheet})_2$ as $GSL_{N\times2}$. The GSLs constructed with either armchair or zigzag interfaces are represented as ac-$GSL_{N\times2}$ or zz-$GSL_{N\times2}$, respectively. All possible 2D $GSL_{N\times2}$ can be further divided into four representative crystal structures of $GSL_{N\times2}$, as shown in Figure 2a-d. The first two structures of ac-$GSL_{N\times2}$ have the armchair interfaces with N = 3 (Figure 2a) and 4 (Figure 2b), respectively. The other two structures of zz-$GSL_{N\times2}$ have zigzag interfaces with N = 3 (Figure 2c) and 4 (Figure 2d), respectively. Figure 2a,c represents odd number of N, and Figure 2b,d indicates the even number of N, respectively.

Pza-C_{10} sheet is semiconducting, whereas pristine graphene is semimetallic at the Dirac point, and it is natural to ask which kind of electronic properties these $GSL_{N\times2}$ will inherit from graphene and pza-C_{10}. To explore the possible electronic structure of such 2D GSLs, the band structures of the different width of $GSL_{N\times2}$ are further calculated. As shown in Figure 2g−n, interestingly, the electronic band structures of $GSL_{N\times2}$ show three different states of metallic, semimetallic at the Dirac point, and semiconducting (indirect band gap) features for the distinct 2D GSLs. This indicates that the $GSL_{N\times2}$ can provide various different types of electronic properties through the combinations of zigzag or armchair interfaces and the number of zigzag or armchair chains (N). That is to say, the GSLs can inherit the character from either graphene or pza-C_{10}, and the electronic properties greatly depend on the atomic configurations.

The variations of the band gap as a function of the number (N) of armchair or zigzag chains in the $GSL_{N\times2}$ unit cell are shown in Figure 3. It is found that the band gaps show different features as a function of the number of graphene. For the ac-$GSL_{N\times2}$, it exhibits the metallic and semiconducting (indirect band gap) features. (See Figure 2g−j for N = 1−4.) The

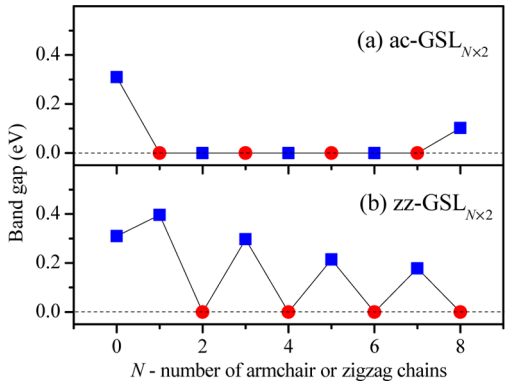

Figure 3. Variation of the band gap calculated with PBE functional as a function of the chain number, N, for the different chirality: ac-$GSL_{N\times2}$ (a) and zz-$GSL_{N\times2}$ (b). The band gap at N = 0 is for the pza-C_{10} sheet. The band gaps represented by blue boxes are calculated from the blue Brillouin zone, whereas the red boxes correspond to the red Brillouin zone. The maximum band gap of 0.40 eV with PBE functional is located when N = 1 in zz-$GSL_{N\times2}$.

maximum band gap among the ac-$GSL_{N\times2}$ is <0.2 eV with PBE functional, as shown in Figure 3a. Different from ac-$GSL_{N\times2}$, it is quite unexpected that the band gaps of zz-$GSL_{N\times2}$ show an oscillation feature as a function of the number of graphene. As shown in Figure 3b, the band gaps of zz-$GSL_{N\times2}$ give oscillation between zero band gaps for even N and indirect band gaps for odd N. The oscillation periodicity of the band gap for the zz-$GSL_{N\times2}$ as a function of the number (N) is about the width of two graphene unit cell (N = 2), corresponding to a width of ∼4.3 Å.

In fact, such different kinds of oscillations are related to the distinct symmetry for the armchair and zigzag type of $GSL_{N\times2}$. Although all four representative crystal structures of $GSL_{N\times2}$ shown in Figure 2a-d have the symmetry of $P2/M$ (no. 10), two different types of Brillouin zones (BZs) exist in these structures because of different cell angles. The first type of BZ is marked with blue solid lines (Figure 2e). The ac-$GSL_{N\times2}$ with even N (Figure 2b) and the zz-$GSL_{N\times2}$ with odd N (Figure 2c) possess this symmetry. The second type of BZ is marked with red solid lines (Figure 2f). The ac-$GSL_{N\times2}$ with odd N (Figure 2a) and zz-$GSL_{N\times2}$ with even N (Figure 2d) have this kind of symmetry. The first type of BZ in $GSL_{N\times2}$ shows the shape of irregular hexagon, whereas the second type BZ in $GSL_{N\times2}$ exhibits the shape of a rectangle. The BZ oscillations exist for both armchair and zigzag $GSL_{N\times2}$. As shown in Figure 3, the odd−even oscillations for the band gap of $GSL_{N\times2}$ exist only in zz-$GSL_{N\times2}$. Therefore, it can be inferred that the special symmetry for 2D zz-$GSL_{N\times2}$ should not be the only reason for the odd−even oscillation for the band gap of zz-$GSL_{N\times2}$. The zigzag type of chains and the width of graphene in zz-$GSL_{N\times2}$ should also be related to the band gap oscillations.

One further important result should be noticed that the band structures of the zz-$GSL_{N\times2}$ with zero band gaps (even N) have a common feature of Dirac point (for example, see Figure 2l,n). It is should also be noted that most of ac-$GSL_{N\times2}$ have the metallic feature. Although it was thought that graphene has Dirac point because of hexagonal symmetry, recent theoretical calculations suggested that 6,6,12-graphyne with nonhexagonal symmetry also has the electronic properties of Dirac point.[29] Interestingly, the 2D superlattice of zz-$GSL_{N\times2}$ with even number of N also exhibits the amazing electronic properties of Dirac point.

dx.doi.org/10.1021/jz301325z | J. Phys. Chem. Lett. 2012, 3, 3373−3378

The maximum band gap of 0.40 eV with PBE appears at N = 1 for the zz-GSL$_{N\times2}$. The band gap of the maximum is ∼0.1 eV larger than the pure pza-C$_{10}$. It is well known that the normal GGA functional usually underestimates the band gap of semiconductor because of the self-interaction error. As discussed above, the band gap of pza-C$_{10}$ is 0.31 eV with PBE. To calculate accurately the band gap of the pza-C$_{10}$, the hybrid functional HSE06 was used, which has shown that it can reproduce the well band gap of the semiconductor.[34] The calculated band gap of pza-C$_{10}$ with HSE06 is 0.71 eV, which is ∼0.4 eV larger than that of PBE. The maximum band gap of GSLs comes from the zz-GSL$_{1\times2}$, which is 0.40 eV with PBE functional. Considering that the band gap of zz-GSL$_{1\times2}$ is ∼0.1 eV larger than that of pza-C$_{10}$, it can thus be expected that the band gap of zz-GLS$_{1\times2}$ may be ∼0.8 eV with hybrid functional, which is close to the band gap of silicon.

The present oscillation of the band gaps is clearly different from that in GNR.[13,15] The typical feature of GNR is that band gap decreases with increasing nanoribbon width,[13,15] which origins from the gradual reduction of the edge effects on the system. GSL$_{N\times2}$ can also be considered to be periodic line defects in graphene (Figure 2a−d), similar to the reported metallic line defects of 5−8−5−8 rings in graphene, as observed in the experiment.[35] Increasing N in the unit cells of the GSL$_{N\times2}$ is identical to decreasing the density of the line defects in graphene. Because these line defects provide the GSL$_{N\times2}$ certain band gaps, lower density of line defects will naturally result in the reduction of their band gaps. It is expected that the physical properties of zz-GSL$_{N\times2}$ will recover to those of graphene when N is large enough.

In summary, a novel carbon allotrope, pza-C$_{10}$ sheet, with an indirect band gap of 0.31 eV with PBE and 0.71 eV with HSE06 was discovered. The pza-C$_{10}$ sheet is energetically more stable than the previously predicted or fabricated semiconducting carbon sheets and fullerene C$_{60}$. The pza-C$_{10}$ sheet contains parallel armchair and zigzag chains, which provides the possibility to perfectly graft with graphene to form 2D superlattice. A series of GSLs can be constructed by combining pza-C$_{10}$ sheet with graphene, forming interfaces with armchair or zigzag chains. The metallic, semimetallic at the Dirac point, and semiconducting features can be amazingly tuned through changing the width of GSLs. As N increases in the zz-GSL$_{N\times2}$ unit cell, the band gaps oscillate between semiconducting and semimetallic (mostly at the Dirac point) states, depending on the odd or even number of zigzag chains. The oscillatory behavior exhibits a typical feature of quantum size effect. Such approaches suggest a new strategy of modulating band gap by forming monolayer carbon superlattices, opening up the new way to design the crystal structures and to adjust physical properties of low-dimensional materials such as 2D materials, nanoribbons, and nanotubes.

CALCULATION METHODS

Structure searches for 2D carbon allotropes were performed using the CALYPSO code[36] with cell size of up to 16 atoms at zero pressure. Structural relaxations were performed based on density functional theory (DFT) with Perdew−Burke−Ernzerhof (PBE) functional,[37] as implemented in the Vienna ab initio simulation package (VASP) code.[38] The all-electron projector-augmented wave method was adopted with $2s^2 2p^2$ treated as valence electrons for carbon. The vacuum zone of 15 Å was used. A plane-wave basis set with an energy cutoff of 500 eV and k points of 0.02 1/Å was used. The structures were fully relaxed until the total energy difference was $<1 \times 10^{-5}$ eV/atom. The molecular dynamics simulation was conducted with the LAMMPS package.[39] The carbon interaction potential is described by ReaxFF reactive force field.[40] Microcanonical ensemble (NVE) simulation was performed with time step of 0.25 fs. A two-dimensionally periodic (infinite) carbon slab containing a total 1000 atoms was thermalized by Berendsen thermostat at 300, 900, 2100, and 3000 K for 25 ps to check the stability of pza-C$_{10}$ sheet.

AUTHOR INFORMATION

Corresponding Author

*E-mail: luoxgg@yahoo.com.

Notes

The authors declare no competing financial interest.

ACKNOWLEDGMENTS

This work was supported by NSFC (grant nos. 50902072, 11104148, 11074128, 51121061, 11244001, 51222212, and 50931003), CAEP foundation (grant no. 2012B0302052), and Shu Guang Project (grant no. 09SG36).

REFERENCES

(1) Novoselov, K. S.; Geim, A. K.; Morozov, S. V.; Jiang, D.; Katsnelson, M. I.; Grigorieva, I. V.; Dubonos, S. V.; Firsov, A. A. Two-Dimensional Gas of Massless Dirac Fermions in Graphene. *Nature (London)* **2005**, *438*, 197−200.

(2) Zhang, Y. B.; Tan, Y. W.; Stormer, H. L.; Kim, P. Experimental Observation of the Quantum Hall Effect and Berry's Phase in Graphene. *Nature (London)* **2005**, *438*, 201−204.

(3) Novoselov, K. S.; McCann, E.; Morozov, S. V.; Fal'ko, V. I.; Katsnelson, M. I.; Zeitler, U.; Jiang, D.; Schedin, F.; Geim, A. K. Unconventional Quantum Hall Effect and Berry's Phase of 2 Pi in Bilayer Graphene. *Nature Phys.* **2006**, *2*, 177−180.

(4) Geim, A. K.; Novoselov, K. S. The Rise of Graphene. *Nat. Mater.* **2007**, *6*, 183−191.

(5) Balog, R.; Jorgensen, B.; Nilsson, L.; Andersen, M.; Rienks, E.; Bianchi, M.; Fanetti, M.; Laegsgaard, E.; Baraldi, A.; Lizzit, S.; et al. Bandgap Opening in Graphene Induced by Patterned Hydrogen Adsorption. *Nat. Mater.* **2010**, *9*, 315−319.

(6) Sofo, J. O.; Chaudhari, A. S.; Barber, G. D. Graphane: A Two-Dimensional Hydrocarbon. *Phys. Rev. B* **2007**, *75*, 153401.

(7) Giovannetti, G.; Khomyakov, P. A.; Brocks, G.; Kelly, P. J.; van den Brink, J. Substrate-Induced Band Gap in Graphene on Hexagonal Boron Nitride: Ab Initio Density Functional Calculations. *Phys. Rev. B* **2007**, *76*, 073103.

(8) Kim, S.; Ihm, J.; Choi, H. J.; Son, Y. W. Origin of Anomalous Electronic Structures of Epitaxial Graphene on Silicon Carbide. *Phys. Rev. Lett.* **2008**, *100*, 176802.

(9) Zhou, S. Y.; Gweon, G. H.; Fedorov, A. V.; First, P. N.; De Heer, W. A.; Lee, D. H.; Guinea, F.; Neto, A. H. C.; Lanzara, A. Substrate-Induced Bandgap Opening in Epitaxial Graphene. *Nat. Mater.* **2007**, *6*, 770−775.

(10) Ohta, T.; Bostwick, A.; Seyller, T.; Horn, K.; Rotenberg, E. Controlling the Electronic Structure of Bilayer Graphene. *Science* **2006**, *313*, 951−954.

(11) Zhang, Y. B.; Tang, T. T.; Girit, C.; Hao, Z.; Martin, M. C.; Zettl, A.; Crommie, M. F.; Shen, Y. R.; Wang, F. Direct Observation of a Widely Tunable Bandgap in Bilayer Graphene. *Nature (London)* **2009**, *459*, 820−823.

(12) Castro, E. V.; Novoselov, K. S.; Morozov, S. V.; Peres, N. M. R.; Dos Santos, J.; Nilsson, J.; Guinea, F.; Geim, A. K.; Neto, A. H. C. Biased Bilayer Graphene: Semiconductor with a Gap Tunable by the Electric Field Effect. *Phys. Rev. Lett.* **2007**, *99*, 216802.

(13) Barone, V.; Hod, O.; Scuseria, G. E. Electronic Structure and Stability of Semiconducting Graphene Nanoribbons. *Nano Lett.* **2006**, *6*, 2748−2754.
(14) Han, M. Y.; Ozyilmaz, B.; Zhang, Y. B.; Kim, P. Energy Band-Gap Engineering of Graphene Nanoribbons. *Phys. Rev. Lett.* **2007**, *98*, 206805.
(15) Yang, L.; Park, C. H.; Son, Y. W.; Cohen, M. L.; Louie, S. G. Quasiparticle Energies and Band Gaps in Graphene Nanoribbons. *Phys. Rev. Lett.* **2007**, *99*, 186801.
(16) Li, X. L.; Wang, X. R.; Zhang, L.; Lee, S. W.; Dai, H. J. Chemically Derived, Ultrasmooth Graphene Nanoribbon Semiconductors. *Science* **2008**, *319*, 1229−1232.
(17) Park, C. H.; Yang, L.; Son, Y. W.; Cohen, M. L.; Louie, S. G. Anisotropic Behaviours of Massless Dirac Fermions in Graphene under Periodic Potentials. *Nat. Phys.* **2008**, *4*, 213−217.
(18) Pedersen, T. G.; Flindt, C.; Pedersen, J.; Mortensen, N. A.; Jauho, A. P.; Pedersen, K. Graphene Antidot Lattices: Designed Defects and Spin Qubits. *Phys. Rev. Lett.* **2008**, *100*, 136804.
(19) Bai, J. W.; Zhong, X.; Jiang, S.; Huang, Y.; Duan, X. F. Graphene Nanomesh. *Nat. Nanotechnol.* **2010**, *5*, 190−194.
(20) Tsu, R. *Superlattice to Nanoelectronics*; Elsevier: Oxford, U.K., 2010.
(21) Esaki, L.; Tsu, R. Superlattice and Negative Differential Conductivity in Semiconductors. *IBM J. Res. Dev.* **1970**, *14*, 61−65.
(22) Crespi, V. H.; Benedict, L. X.; Cohen, M. L.; Louie, S. G. Prediction of a Pure-Carbon Planar Covalent Metal. *Phys. Rev. B* **1996**, *53*, 13303−13305.
(23) Terrones, H.; Terrones, M.; Hernandez, E.; Grobert, N.; Charlier, J. C.; Ajayan, P. M. New Metallic Allotropes of Planar and Tubular Carbon. *Phys. Rev. Lett.* **2000**, *84*, 1716−1719.
(24) Deza, M.; Fowler, P. W.; Shtogrin, M.; Vietze, K. Pentaheptite Modifications of the Graphite Sheet. *J. Chem. Inf. Comput. Sci.* **2000**, *40*, 1325−1332.
(25) Appelhans, D. J.; Lin, Z. B.; Lusk, M. T. Two-Dimensional Carbon Semiconductor: Density Functional Theory Calculations. *Phys. Rev. B* **2010**, *82*, 073410.
(26) daSilva-Araujo, J.; Chacham, H.; Nunes, R. W. Gap Opening in Topological-Defect Lattices in Graphene. *Phys. Rev. B* **2010**, *81*, 193405.
(27) Enyashin, A. N.; Ivanovskii, A. L. Graphene Allotropes. *Phys. Status Solidi B* **2011**, *248*, 1879−1883.
(28) Luo, G. F.; Qian, X. M.; Liu, H. B.; Qin, R.; Zhou, J.; Li, L. Z.; Gao, Z. X.; Wang, E. G.; Mei, W. N.; Lu, J.; et al. Quasiparticle Energies and Excitonic Effects of the Two-Dimensional Carbon Allotrope Graphdiyne: Theory and Experiment. *Phys. Rev. B* **2011**, *84*, 075439.
(29) Malko, D.; Neiss, C.; Viñes, F.; Görling, A. Competition for Graphene: Graphynes with Direction-Dependent Dirac Cones. *Phys. Rev. Lett.* **2012**, *108*, 086804.
(30) Stone, A. J.; Wales, D. J. Theoretical Studies of Icosahedral C60 and Some Related Species. *Chem. Phys. Lett.* **1986**, *128*, 501−503.
(31) Li, L.; Reich, S.; Robertson, J. Defect Energies of Graphite: Density-Functional Calculations. *Phys. Rev. B* **2005**, *72*, 184109.
(32) Meyer, J. C.; Kisielowski, C.; Erni, R.; Rossell, M. D.; Crommie, M. F.; Zettl, A. Direct Imaging of Lattice Atoms and Topological Defects in Graphene Membranes. *Nano Lett.* **2008**, *8*, 3582−3586.
(33) Banhart, F.; Kotakoski, J.; Krasheninnikov, A. V. Structural Defects in Graphene. *ACS Nano* **2011**, *5*, 26−41.
(34) Jain, M.; Chelikowsky, J. R.; Louie, S. G. Reliability of Hybrid Functionals in Predicting Band Gaps. *Phys. Rev. Lett.* **2011**, *107*, 216806.
(35) Lahiri, J.; Lin, Y.; Bozkurt, P.; Oleynik, I. I.; Batzill, M. An Extended Defect in Graphene as a Metallic Wire. *Nat. Nanotechnol.* **2010**, *5*, 326−329.
(36) Wang, Y. C.; Lv, J. A.; Zhu, L.; Ma, Y. M. Crystal Structure Prediction Via Particle-Swarm Optimization. *Phys. Rev. B* **2010**, *82*, 094116.
(37) Perdew, J. P.; Burke, K.; Ernzerhof, M. Generalized Gradient Approximation Made Simple. *Phys. Rev. Lett.* **1996**, *77*, 3865−3868.
(38) Kresse, G.; Furthmuller, J. Efficient Iterative Schemes for Ab Initio Total-Energy Calculations Using a Plane-Wave Basis Set. *Phys. Rev. B* **1996**, *54*, 11169−11186.
(39) Plimpton, S. Fast Parallel Algorithms for Short-Range Molecular Dynamics. *J. Comput. Phys.* **1995**, *117*, 1−19.
(40) Chenoweth, K.; van Duin, A. C. T.; Goddard, W. A. Reaxff Reactive Force Field for Molecular Dynamics Simulations of Hydrocarbon Oxidation. *J. Phys. Chem. A* **2008**, *112*, 1040−1053.